

LETTER • OPEN ACCESS

Observed and simulated local climate responses to tropical deforestation

To cite this article: Callum Smith *et al* 2023 *Environ. Res. Lett.* **18** 104004

View the [article online](#) for updates and enhancements.

You may also like

- [Deforestation displaced: trade in forest-risk commodities and the prospects for a global forest transition](#)
Florence Pendrill, U Martin Persson, Javier Godar et al.
- [Forest loss in Brazil increases maximum temperatures within 50 km](#)
Avery S Cohn, Nishan Bhattarai, Jake Campolo et al.
- [Forest loss is significantly higher near clustered small dams than single large dams per megawatt of hydroelectricity installed in the Brazilian Amazon](#)
Samuel Nickerson, Gang Chen, Philip M Fearnside et al.

ENVIRONMENTAL RESEARCH
LETTERS

LETTER

Observed and simulated local climate responses to tropical deforestation

OPEN ACCESS

RECEIVED
18 May 2023REVISED
7 August 2023ACCEPTED FOR PUBLICATION
16 August 2023PUBLISHED
15 September 2023

Original content from this work may be used under the terms of the [Creative Commons Attribution 4.0 licence](#).

Any further distribution of this work must maintain attribution to the author(s) and the title of the work, journal citation and DOI.



Callum Smith^{1,*} , Eddy Robertson² , Robin Chadwick² , Douglas I Kelley³ , Arthur P K Argles² , Caio A S Coelho⁴ , Dayana C de Souza⁴ , Paulo Y Kubota⁴ , Isabela L Talamoni⁴ , Dominick V Spracklen¹  and Jessica C A Baker^{1,*} 

¹ School of Earth and Environment, University of Leeds, Leeds LS2 9JT, United Kingdom

² Met Office Hadley Centre, FitzRoy Road, Exeter EX1 3PB, United Kingdom

³ UK Centre for Ecology and Hydrology, Wallingford OX10 8BB, United Kingdom

⁴ Centro de Previsão de Tempo e Estudos Climáticos (CPTEC), Instituto Nacional de Pesquisas Espaciais (INPE), Rodovia Presidente Dutra, Km 40, SP-RJ, Cachoeira Paulista, SP 12630-000, Brazil

* Authors to whom any correspondence should be addressed.

E-mail: C.M.Smith1@leeds.ac.uk and J.C.Baker@leeds.ac.uk

Keywords: observed, simulated, climate, responses, tropical, deforestations, CMIP6

Supplementary material for this article is available [online](#)

Abstract

Tropical deforestation has local and regional effects on climate, but the sign and magnitude of these effects are still poorly constrained. Here we used satellite observations to evaluate the local land surface temperature and precipitation response to tropical deforestation in historical simulations from 24 CMIP6 models. We found tropical forest loss leads to an observed local dry season warming and reduced wet and dry season precipitation across the range of scales (0.25°–2°) analysed. At the largest scale analysed (2°), we observed a warming of 0.018 ± 0.001 °C per percentage point of forest loss (°C %⁻¹), broadly captured in the multi-model mean response of 0.017 ± 0.005 °C %⁻¹. The multi-model mean correctly simulates reduced precipitation due to forest loss in the dry season but simulates increased precipitation due to forest loss in the wet season, opposite to the observed response. We found that the simulated dry season surface temperature and precipitation changes due to forest loss depend on the simulated surface albedo change, with less warming and less drying in models with greater increases in surface albedo due to forest loss. Increased recognition of the local and regional climate benefits of tropical forests is needed to support sustainable land use policy.

1. Introduction

Land cover change alters energy and water fluxes between the surface and atmosphere affecting the local and regional climate (Bonan 2008, Pongratz *et al* 2021). Tropical regions are experiencing rapid changes to land cover, particularly from deforestation (Hansen *et al* 2013) and forest degradation (Vancutsem *et al* 2021). Tropical deforestation has been shown to cause local surface warming of greater than 2 °C (Alkama and Cescatti 2016, Bright *et al* 2017, Duveiller *et al* 2018, Baker and Spracklen 2019). The effect on precipitation is more complex and scale-dependent (Lawrence and Vandecar 2015),

with increases in precipitation over or near small-scale deforestation (Garcia-Carreras and Parker 2011, Khanna *et al* 2017, Taylor *et al* 2022) and reductions over and downwind of large-scale deforestation (Spracklen and Garcia-Carreras 2015). Analysis of remotely sensed precipitation suggests tropical forest loss causes reductions in local precipitation, particularly at scales larger than 50 km (Smith *et al* 2023).

Climate models have different representations of the land surface and the biophysical responses to land cover change, leading to different simulations of the climate response to land cover change (Boisier *et al* 2015, Boysen *et al* 2020, Baker *et al* 2021a, Luo *et al* 2022, De Hertog *et al* 2023). Most models agree that

deforestation in the tropics causes local surface warming but disagree on the magnitude of the temperature response (Winckler *et al* 2019b, Boysen *et al* 2020). In contrast, some models simulate local cooling over tropical deforestation due to strong increases in simulated surface albedo (Robertson 2019). The simulated response of local precipitation to land cover change is even more varied. Luo *et al* (2022) simulated the impacts of idealised deforestation scenarios and found a multi-model mean reduction in precipitation over regions of forest loss of -2.2% , with a range of -5.5% to $+0.1\%$ across 11 models. Spracklen and Garcia-Carreras (2015) synthesised simulated impacts of deforestation in the Amazon basin, finding an average of $12 \pm 11\%$ reduction in annual precipitation due to basin-wide deforestation.

Previous assessments of climate model responses to land cover change have analysed both idealised (e.g. Davin and de Noblet-ducoustre 2010, Winckler *et al* 2017, Boysen *et al* 2020, Luo *et al* 2022) and historical (De Noblet-Ducoudré *et al* 2012, Kumar *et al* 2013, Lejeune *et al* 2017) land cover scenarios. Evaluation of simulated climate impacts against observations (Duveiller *et al* 2018) have largely focused on temperature from satellite (Li *et al* 2015, Alkama and Cescatti 2016, Bright *et al* 2017, Duveiller *et al* 2018) or *in-situ* measurements (Lee *et al* 2011). Simulations of the impacts of land cover change on precipitation (Luo *et al* 2022) have not yet fully been evaluated. We build on this previous work by evaluating the impacts of tropical deforestation in the historical CMIP6 simulations on both local land surface temperature (T) and precipitation (P) in a consistent manner. We focus on tropical deforestation because of the urgent need for clear evidence to support conservation of remaining tropical forests for climate change adaptation and mitigation (Windisch *et al* 2021). We explore how the climate sensitivity to the extent of forest loss depends on simulated changes to surface albedo, evapotranspiration (ET), and leaf area index (LAI). We evaluate the simulated response using satellite observations, applying a before-after-control-impact approach, where the change in local climate over regions of forest loss is compared against the change in climate over control areas with no forest loss. This allows us to analyse the simulated and observed responses to deforestation identically.

2. Data and methods

We analysed data from 24 CMIP6 models (CMIP6 Tier 1: historical; dataset information listed in table 1), with spatial resolution varying from 0.56 to 2.79 degrees latitudinally. We downloaded and processed monthly mean surface albedo, ET, LAI, land surface temperature and precipitation for 1850–2014.

To evaluate the CMIP6 models, we used satellite data from the period 2003–2019. We calculated forest

loss from the Global Forest Change (GFC) version 1.9 (Hansen *et al* 2013), using forest canopy cover in 2000 and subsequent annual forest loss from 2003 to 2019 at 30 metre (m) resolution. We used MODIS albedo (MCD43A3), ET (MOD16A2GF) and LAI (MOD15A2) available at 500 m resolution and land surface temperature day-night mean (MOD11C3) available at 1 km resolution. We used precipitation data from nine datasets, spanning a range of native resolutions from ~ 4 to 25 km (approx. at equator, table 1 lists the details).

We analysed the observed impacts of forest loss across four spatial scales ($0.25^\circ \times 0.25^\circ$, $0.5^\circ \times 0.5^\circ$, $1.0^\circ \times 1.0^\circ$ and $2.0^\circ \times 2.0^\circ$), spanning the spatial resolution of the CMIP6 models. We performed spatial regridding using the Python package Iris (Met Office 2023) with the area-weighted regridding scheme. Datasets were regridded to coarser resolutions using the highest available resolution as listed in table 1. Two alternative regridding methods (xESMF (Zhuang 2022): ‘conservative-normalised’ and ‘bilinear’) were tested and had little impact on our results. We calculated forest loss at each spatial resolution as the sum of all 30 m pixels within each larger pixel.

We constrained our analysis to the tropics (30° S– 30° N). We additionally constrained satellite datasets by the tropical evergreen broadleaf biome, defined by the MODIS land cover dataset (MCD12Q1), and CMIP6 models by areas where their forest cover was greater than 70% at the start of the discrete analysis periods. This accounted for the fact that simulated forests may be in different geographical areas within each model. We tested both constraining CMIP6 models by MODIS evergreen broadleaf and by areas of forest cover greater than 70%, finding similar results with both methods. We analysed separately over the Amazon and Congo Basins and southeast Asia using shapefiles to geographically constrain the analysis as outlined in supplementary figure 1.

Detecting a robust local climate response to deforestation requires long simulations (Winckler *et al* 2017). For this reason, we analysed data over 16 year periods. For the satellite datasets, this period was 2003–2019, as this was the longest common period of precipitation data. For the CMIP6 models, we analysed ten 16 year periods starting in 1854 and ending in 2014. We selected 16 year periods to match the length of the satellite record and report model values as the median across the ten periods. In addition to this, we analysed the CMIP6 models over five 32 year periods, finding similar results over this longer time period (supplementary figures 2–5). To reduce the impact of interannual variability in temperature and precipitation, we compared 5 year means at the start and end of each analysis period.

Land cover change causes both local and non-local climate impacts (Pongratz *et al* 2021). The local climate impacts of land cover change can be assessed

Table 1. CMIP6 model and satellite datasets used in this analysis. Models are grouped by spatial resolution ($<1^\circ$, and $\geq 1^\circ$ resolution in latitude).

Dataset	Institute	Resolution lon, lat (degrees)	Resolution grouping	Reference
Model				
ACCESS-ESM1-5	CSIRO	1.88×1.25	$>1^\circ$	(Ziehn <i>et al</i> 2019)
AWI-ESM-1-1-LR	AWI	1.88×1.87	$>1^\circ$	(Danek <i>et al</i> 2020)
CanESM5	CCCma	2.81×2.79	$>1^\circ$	(Swart <i>et al</i> 2019a)
CanESM5-CanOE	CCCma	2.81×2.79	$>1^\circ$	(Swart <i>et al</i> 2019b)
CESM2	NCAR	1.25×0.94	$<1^\circ$	(Danabasoglu 2019a)
CESM2-FV2	NCAR	2.50×1.89	$>1^\circ$	(Danabasoglu 2019b)
CESM2-WACCM	NCAR	1.25×0.94	$<1^\circ$	(Danabasoglu 2019c)
CESM2-WACCM-FV2	NCAR	2.50×1.89	$>1^\circ$	(Danabasoglu 2019d)
CMCC-CM2-SR5	CMCC	1.25×0.94	$<1^\circ$	(Lovato and Peano 2020)
CMCC-ESM2	CMCC	1.25×0.94	$<1^\circ$	(Lovato <i>et al</i> 2021)
CNRM-ESM2-1	CNRM-CERFACS	1.41×1.40	$>1^\circ$	(Seferian 2018)
EC-Earth3-CC	EC-Earth-Consortium	0.70×0.70	$<1^\circ$	(EC-Earth-Consortium 2021)
EC-Earth3-Veg	EC-Earth-Consortium	0.70×0.70	$<1^\circ$	(EC-Earth-Consortium 2019)
EC-Earth3-Veg-LR	EC-Earth-Consortium	1.12×1.12	$>1^\circ$	(EC-Earth-Consortium 2020)
GISS-E2-1-G	NASA-GISS	2.50×2.00	$>1^\circ$	(NASA/GISS 2018)
HadGEM3-GC31-LL	MOHC	1.88×1.25	$>1^\circ$	(Ridley <i>et al</i> 2019)
HadGEM3-GC31-MM	MOHC	0.83×0.56	$<1^\circ$	(Ridley <i>et al</i> 2019)
INM-CM4-8	INM	2.00×1.50	$>1^\circ$	(Volodin <i>et al</i> 2019a)
INM-CM5-0	INM	2.00×1.50	$>1^\circ$	(Volodin <i>et al</i> 2019b)
IPSL-CM5A2-INCA	IPSL	3.75×1.89	$>1^\circ$	(Boucher <i>et al</i> 2018)
IPSL-CM6A-LR	IPSL	2.50×1.27	$>1^\circ$	(Boucher <i>et al</i> 2018)
MPI-ESM-1-2-HAM	HAMMOZ-Consortium	1.88×1.87	$>1^\circ$	(Neubauer <i>et al</i> 2019)
MPI-ESM1-2-HR	MPI-M	0.94×0.94	$<1^\circ$	(Jungclaus <i>et al</i> 2019)
UKESM1-0-LL	MOHC	1.88×1.25	$>1^\circ$	(Tang <i>et al</i> 2019)
Satellite				
MODIS Albedo (MCD43A3)		0.05×0.05	n/a	(Schaaf and Wang 2021)
MODIS Evapotranspiration (MOD16A2)		0.05×0.05	n/a	(Running <i>et al</i> 2021)
MODIS Leaf Area Index (MOD15A2)		0.05×0.05	n/a	(Myneni <i>et al</i> 2021)
MODIS Land Surface Temperature (MOD11A2)		0.05×0.05	n/a	(Wan <i>et al</i> 2021)
MODIS Land Cover Type (MCD12Q1)		0.05×0.05	n/a	(Friedl and Sulla-Menashe 2022)
CHIRPS Precipitation (CHIRPS-2.0)		0.05×0.05	n/a	(Funk <i>et al</i> 2015)
CMORPH		0.25×0.25	n/a	(Xie <i>et al</i> 2019)
GPCP v3.2		0.5×0.5	n/a	(Huffman <i>et al</i> 2022)
GPM v0.6		0.1×0.1	n/a	(Hou <i>et al</i> 2014)
PERSIANN-CCS		0.04×0.04	n/a	(Nguyen <i>et al</i> 2019)
PERSIANN-CDR		0.25×0.25	n/a	(Ashouri <i>et al</i> 2015)
PERSIANN-CCSCDR		0.04×0.04	n/a	(Sadeghi <i>et al</i> 2021)
PERSIANN		0.25×0.25	n/a	(Nguyen <i>et al</i> 2019)
TRMM v3B43		0.25×0.25	n/a	(Huffman <i>et al</i> 2007)
Global Forest Change (GFC v1.9)		$30 \text{ m} \times 30 \text{ m}$	n/a	(Hansen <i>et al</i> 2013)

from a single simulation through comparing the climate change over regions of land cover change compared to neighbouring regions with little or no land cover change (Kumar *et al* 2013, Lejeune *et al* 2017). Comparing the change over a pixel with forest loss with its immediate neighbour with little or no forest loss removes the impacts of climate change and variability. We adopted this approach and analysed the local climate response to forest loss using a moving

window nearest neighbour approach as used by previous studies (Baker and Spracklen 2019, Smith *et al* 2023), here employing a 3×3 grid size. We calculated the forest loss of each deforested pixel relative to neighbouring control pixels as the forest loss of the deforested pixel minus the forest loss of the control. To be included in the analysis, deforested pixels must have experienced more than 0.1 percentage points of forest loss compared to their neighbouring

control pixels. We calculated the change in each variable over the deforested pixel relative to the change of the control pixel. We report changes as a function of forest loss by dividing by the difference in forest loss between deforested and control pixels.

We focused our temperature analysis on the dry season, where there was better availability of satellite data for albedo, ET, LAI, and T, as the wet season has more clouds which obstruct satellite retrievals. Dry season temperature is also more sensitive to tropical deforestation (Baker and Spracklen 2019). For precipitation, we analysed dry, wet and transition seasons as the driest 3 months, wettest 3 months and remaining 6 months, respectively, of each year for each pixel. The satellite remotely sensed precipitation value is based on the median of the nine satellite precipitation datasets, whilst for the CMIP6 models, we derived each model's season from its own precipitation data.

To test the relationships between climate variables, we fitted linear regressions using Pearson's correlation coefficient, (calculated using SciPy (Virtanen *et al* 2020)) to identify whether the computed correlation coefficients were found to be statistically significant and different from zero at the 5% level ($p < 0.05$). We report errors throughout as the standard error of the mean.

3. Results and discussion

Figure 1 shows the observed impacts of forest loss on local land surface temperature and precipitation. We observed dry season warming due to forest loss across all spatial scales analysed (figure 1(a)). This demonstrates that tropical forest loss caused local warming at spatial scales simulated in regional ($0.25^\circ \times 0.25^\circ$, $\sim 25 \text{ km} \times 25 \text{ km}$) to global ($2.0^\circ \times 2.0^\circ$, $\sim 200 \text{ km} \times 200 \text{ km}$) climate models. Warming varies from $0.009 \pm 0.002 \text{ }^\circ\text{C } \%^{-1}$ (median \pm standard error of the mean) at $1.0^\circ \times 1.0^\circ$ to $0.018 \pm 0.001 \text{ }^\circ\text{C } \%^{-1}$ at $2.0^\circ \times 2.0^\circ$. The local land surface warming we report here is similar to previous studies such as Alkama and Cescatti (2016) who reported that tropical forest deforestation caused a warming of $0.015 \pm 0.001 \text{ }^\circ\text{C } \%^{-1}$. Duveiller *et al* (2020) used a space-for-time approach and reported a warming of $0.018 \pm 0.001 \text{ }^\circ\text{C } \%^{-1}$ for wet tropical forests using $1.0^\circ \times 1.0^\circ$ resolution data. In the Amazon, Baker and Spracklen (2019) reported deforestation caused dry season land surface warming of $0.014 \text{ }^\circ\text{C } \%^{-1}$ using 0.05° resolution data.

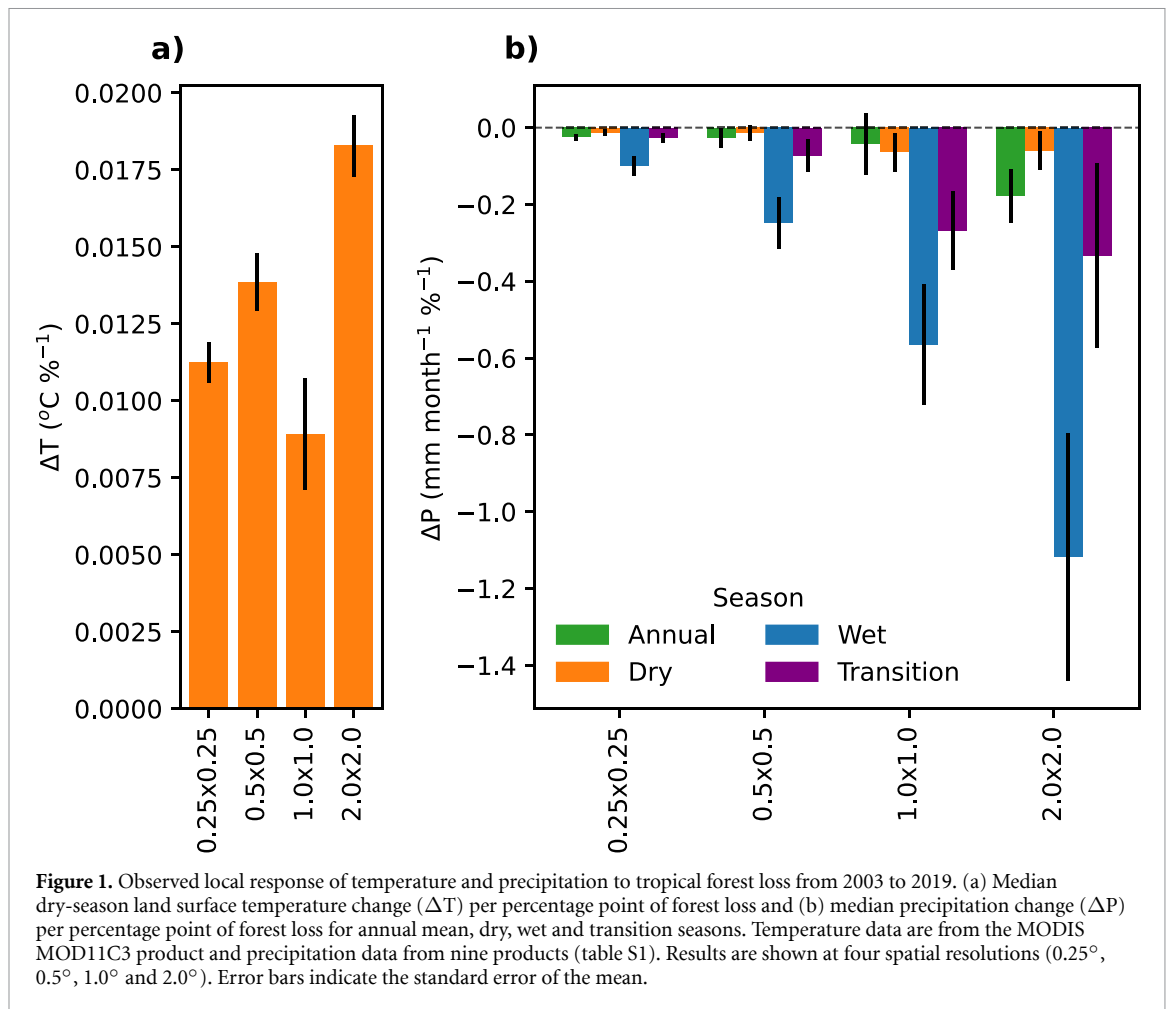
We observed reductions in precipitation over regions of tropical forest loss at both an annual scale and in the dry, wet and transition seasons (figure 1(b)). Forest loss causes a decrease in precipitation across all analysed resolutions, with larger reductions as the scale of forest loss increases. At 2° resolution, the annual reduction was $-0.18 \pm 0.07 \text{ mm month}^{-1} \%^{-1}$. This sensitivity

is slightly lower than reported by Smith *et al* (2023) ($-0.25 \pm 0.10 \text{ mm month}^{-1} \%^{-1}$ at 2°) due to small methodological differences, including a longer analysis period (2003–2019 compared to 2003–2017). Reductions in precipitation were observed throughout the year, with the largest absolute reductions in precipitation over regions of forest loss in the wet season ($-1.12 \pm 0.32 \text{ mm month}^{-1} \%^{-1}$) compared to $-0.06 \pm 0.05 \text{ mm month}^{-1} \%^{-1}$ in the dry season and $-0.33 \pm 0.24 \text{ mm month}^{-1} \%^{-1}$ in the transition season.

Figure 2 compares the simulated and observed impact of forest loss on local dry season land surface temperature. Most models (22 out of 24) simulate a warming response consistent with the satellite observations. The simulated surface temperature response to forest loss varies from $-0.038 \pm 0.008 \text{ }^\circ\text{C } \%^{-1}$ (GISS-E2-1-G) to $+0.042 \pm 0.009 \text{ }^\circ\text{C } \%^{-1}$ (CESM2-WACCM-FV2). In idealised deforestation simulations, Boysen *et al* (2020) found that the near-surface air temperature response simulated by CMIP6 models varied between $-0.02 \text{ }^\circ\text{C } \%^{-1}$ and $+0.08 \text{ }^\circ\text{C } \%^{-1}$.

The local surface warming due to forest loss is relatively insensitive to spatial scale, both in the models and observations. The multi-model mean warming due to forest loss is $+0.017 \pm 0.005 \text{ }^\circ\text{C } \%^{-1}$ ($0.016 \pm 0.002 \text{ }^\circ\text{C } \%^{-1}$ for models $< 1^\circ$ resolution and $0.017 \pm 0.006 \text{ }^\circ\text{C } \%^{-1}$ for models $> 1^\circ$ resolution), which compares well to the observed warming of $0.018 \pm 0.001 \text{ }^\circ\text{C } \%^{-1}$ (at 2° resolution). Whilst the multi-model mean is close to the observed value, figure 2 highlights the large variability across models. We also analysed the simulated temperature change due to forest loss for each model separately over the ten 16 year model periods (supplementary figure 6). Only 7 models show consistent warming across all periods. Most models (17 out of 24) show warming and cooling in different periods, five of which (CanESM5, CMCC-ESM2, GISS-E2-1-G, MPI-ESM1-2-HR and UKESM1-0-LL) show a cooling response in four or more of the ten 16 year periods contrary to the observed temperature response. This further confirms the need for long simulations to robustly diagnose a climate response to land use change from climate models. When analysing the simulated temperature change over the longer 32 year periods (supplementary figure 2), we find a very similar multi-model mean warming response of $0.019 \pm 0.004 \text{ }^\circ\text{C } \%^{-1}$. Most models show a consistent warming in both the 16 year and 32 year analysis (supplementary figures 3 and 7), with only GISS-E2-1-G and MPI-ESM1-2-HR showing an overall cooling in the 16 year analysis and UKESM1-0-LL and MPI-ESM1-2-HR showing a cooling in the 32 year analysis.

Figure 3 compares the simulated and observed changes in dry and wet season precipitation due to tropical forest loss. The simulated precipitation

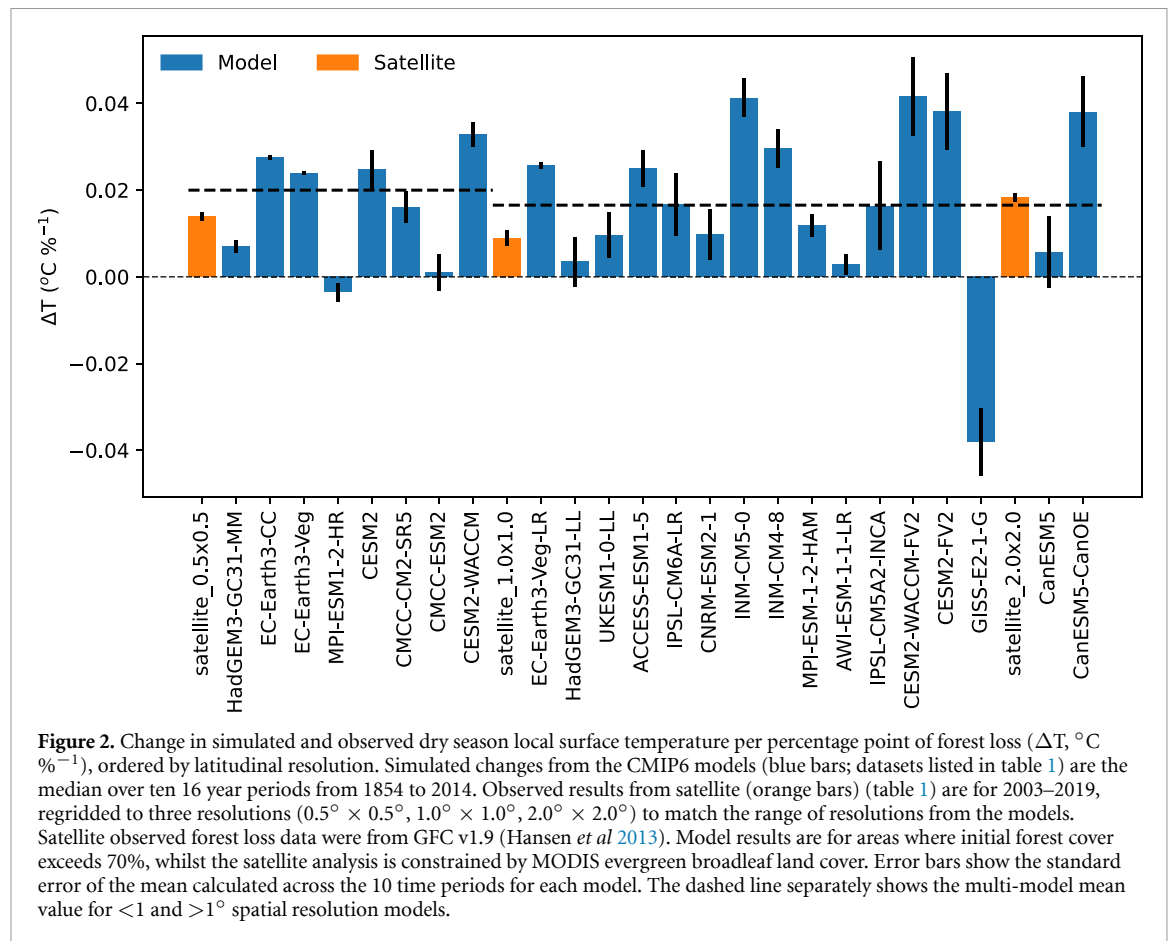


response to forest loss is less consistent than for temperature. In the dry season, 6 of the 24 models simulate increases in precipitation due to forest loss, whilst the remaining 18 models simulate reductions. In the wet season, 10 of the 24 models simulate an increase, whilst the remaining 14 simulate a decrease. Across all models, the multi-model mean response of dry season precipitation to forest loss is $-0.06 \pm 0.08 \text{ mm month}^{-1} \%^{-1}$, comparable to the observed change of $-0.06 \pm 0.05 \text{ mm month}^{-1} \%^{-1}$ (at 2°). The multi-model mean response in the wet season is $0.11 \pm 0.65 \text{ mm month}^{-1} \%^{-1}$, opposite to the observed response of $-1.12 \pm 0.32 \text{ mm month}^{-1} \%^{-1}$. The individual CMIP6 models tend to be oversensitive to forest loss (either large increases or decreases) compared to observed changes. Analysing over 32 years, we find a very similar multi-model dry season precipitation response ($-0.063 \pm 0.073 \text{ mm month}^{-1} \%^{-1}$, supplementary figures 4(a) and 5). In the wet season, where there is large intermodel variability in both analysis periods, the multi-model mean response changes to a slight drying ($-0.010 \pm 0.430 \text{ mm month}^{-1} \%^{-1}$).

At the annual scale, the multi-model mean precipitation sensitivity to forest loss is $+0.06 \pm 0.23\%$

per percentage point of forest loss ($\% \%^{-1}$) (supplementary figure 8), opposite in sign to the observed sensitivity of $-0.12 \pm 0.11\% \%^{-1}$ (at 2°). Previous studies have also reported a wide range in the simulated precipitation response to tropical deforestation. Luo *et al* (2022) reported Amazon deforestation resulted in a regional annual mean precipitation response of -11% to $+2\%$ for a 50% reduction in forest cover, equivalent to -0.18% to $+0.04\%$ per percentage forest loss, with eight out of the 11 models simulating decreased precipitation over regions of forest loss in the western and southern Amazon basin. Spracklen and Garcia-Carreras (2015) reported multi-model mean annual mean sensitivity of $-0.16 \pm 0.13\%$ per percentage point forest loss in the Amazon.

To explore the different regional impacts of forest loss on climate, we analysed the changes in temperature and precipitation (supplementary figures 9 and 10 respectively) across the Amazon, Congo Basin and Southeast Asia. Local dry season warming due to forest loss is seen across all regions in both satellite data and the multi-model mean. The models simulate the greatest sensitivity of temperature to forest loss in the Amazon and Congo, however this is not seen in the satellite data. The observed and simulated response of dry season precipitation



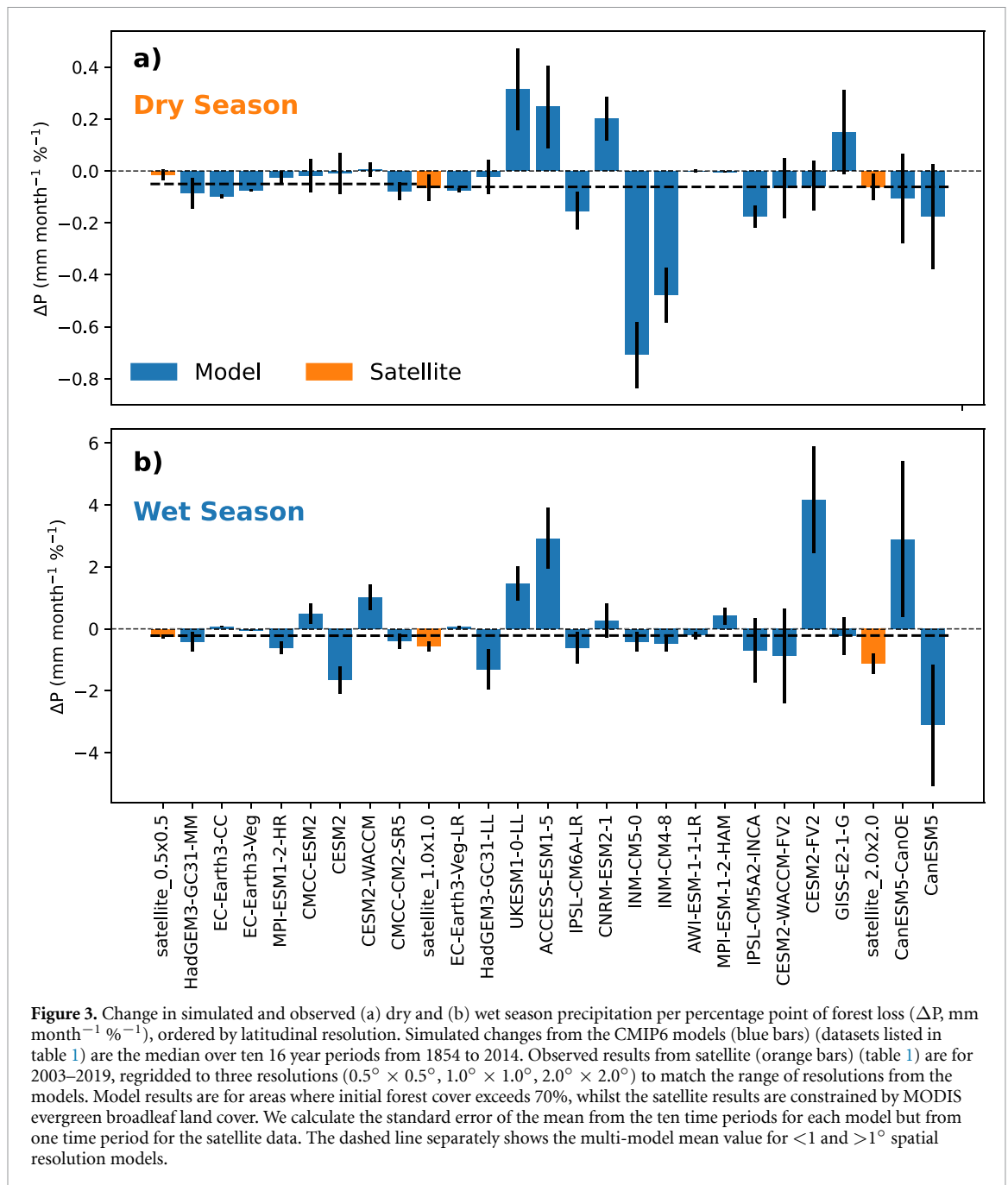
to forest loss is consistent across the tropics as a whole, however regionally the results are divergent, with opposite responses in the Amazon and Congo (supplementary figure 10(a)). In the wet season, there is consistent observed drying due to forest loss across all regions, however in the simulated response, there are increases in precipitation in the Congo and decreases in Southeast Asia (supplementary figure 10(b)). The simulated precipitation responses in the Congo and Southeast Asia have especially large variability, reflecting the divergence of model responses.

Figure 4 compares the median dry season sensitivity of temperature and precipitation to forest cover loss against the equivalent sensitivity of different land surface variables (albedo, ET, LAI) to forest loss. There is substantial variability in the simulated sensitivity of albedo, ET and LAI to forest loss. We find large variability in the simulated sensitivity of surface albedo to forest loss varying from ~ 0 to $5.1 \times 10^{-4} \%^{-1}$, with 23 of the 24 models simulating an increase in surface albedo in regions of forest loss (INM-CM4-8 simulates a decrease). A previous assessment of the CMIP5 models also found large variability in the simulated albedo response to land use change (Lejeune *et al* 2020). For ET, we find simulated sensitivity ranges from -1 to $+0.5 \text{ mm month}^{-1} \%^{-1}$. Luo *et al* (2022) reported that forest loss caused annual mean changes of

$+50$ to $-150 \text{ mm year}^{-1}$. For LAI, we find a simulated sensitivity of -0.05 to $0.03 \text{ m}^2 \text{ m}^{-2} \%^{-1}$. In the Amazon, Luo *et al* (2022) also reported a wide range in the sensitivity of LAI to forest loss ranging from -2 to $+1 \text{ m}^2 \text{ m}^{-2}$, equivalent to -0.02 to $+0.01 \text{ m}^2 \text{ m}^{-2} \%^{-1}$.

The local warming due to forest loss is caused by reduced surface roughness, which reduces turbulent heat fluxes and ET (Bright *et al* 2017, Duveiller *et al* 2018). For dry season temperature, we find statistically significant relationships ($P < 0.05$) with albedo ($r^2 = 0.299$) and ET ($r^2 = 0.292$). As would be expected (Bright *et al* 2017, Duveiller *et al* 2018, Winckler *et al* 2019a), models with a stronger sensitivity of surface albedo (greater surface brightening) and weaker sensitivity of ET (smaller ET decreases) to forest loss tend to show less warming from forest loss.

Albedo measurements from satellite also suggest increased albedo due to forest loss with a sensitivity of 8.0×10^{-5} – $1.31 \times 10^{-4} \%^{-1}$, equivalent to an increase in albedo of 0.008 – 0.013 for complete forest loss (figure 4). This albedo sensitivity to forest loss is relatively well captured by some models (3 simulating albedo within the satellite range), whereas 9 models underestimate ($< 8.0 \times 10^{-5} \%^{-1}$) and 12 overestimate ($> 1.31 \times 10^{-4} \%^{-1}$) the sensitivity. Models that overestimate the albedo sensitivity to forest loss underestimate the warming due to forest loss.



Most models simulate a reduction in ET over forest loss (multi-model mean -0.19 ± 0.06 mm month⁻¹ %⁻¹), although there is large variability across models with a range of -1.17 to $+0.62$ mm month⁻¹ %⁻¹. The sensitivity of ET to forest loss is related to the change in LAI, as has been shown previously (Luo *et al* 2022), with models that simulate larger decreases in LAI tending to simulate larger decreases in ET following forest loss (supplementary figure 11). Forest loss causes a reduction in simulated ET due to the replacement of forests by grasses with lower ET rates, matching the response in idealised deforestation simulations (Boysen *et al* 2020). Increased ET over regions of forest loss in some models (e.g. CESM) may be due to tropical forests being replaced by C4 grasses that are

productive in the moist tropics (Boysen *et al* 2020), whilst in other models (e.g. GISS-E2-1-G) it may be due to increased simulated precipitation over regions of forest loss.

We found significant positive relationships for dry season precipitation with ET ($r^2 = 0.564$) and albedo ($r^2 = 0.176$). Luo *et al* (2022) also reported positive relationships between changes in precipitation and ET due to deforestation. They also found that the inter-model spread in precipitation response to forest loss primarily results from divergent responses of ET. Previous work has also suggested albedo as an important parameter controlling precipitation changes (Dirmeyer and Shukla 1994, Berbet and Costa 2003, Costa *et al* 2007). Dirmeyer and Shukla (1994) found that the local precipitation

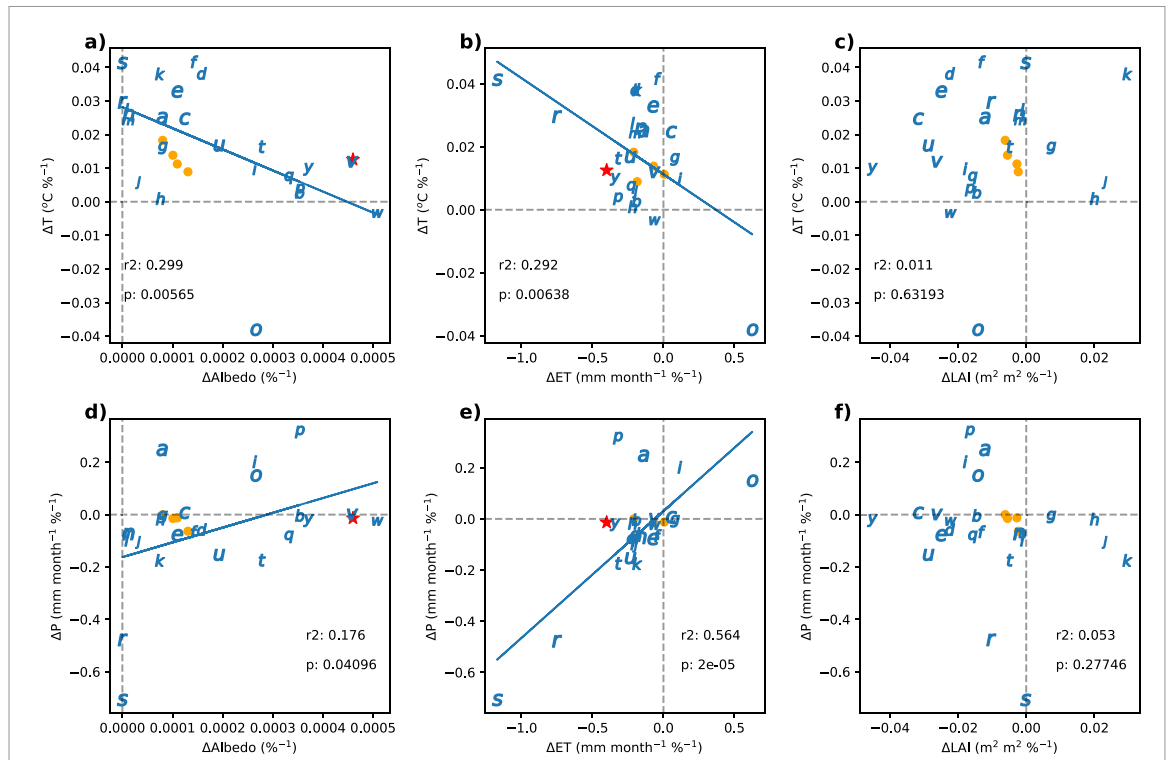


Figure 4. Sensitivity of dry season (a)–(c) land surface temperature (T) and (d)–(f) precipitation (P) to surface albedo (Alb), evapotranspiration (ET), leaf area index (LAI), per percentage point of forest loss. Simulated (blue) values show the median change for each model's ten 16 year periods. We report the linear Pearson correlation coefficient squared (r^2) and the p -value (p) and plot the linear fit where $p < 0.05$. Results are for areas where initial forest cover exceeds 70%. Satellite values are plotted as orange circles, regridded to four resolutions ($0.25^{\circ} \times 0.25^{\circ}$, $0.5^{\circ} \times 0.5^{\circ}$, $1.0^{\circ} \times 1.0^{\circ}$, $2.0^{\circ} \times 2.0^{\circ}$). These values are constrained by MODIS land cover evergreen broadleaf area. The red star indicates *in-situ* measurement from (Culf *et al* 1995, Restrepo-Coupe *et al* 2013). Model key; ACCESS-ESM1-5: 'a', AWI-ESM-1-1-LR: 'b', CESM2: 'c', CESM2-FV2: 'd', CESM2-WACCM: 'e', CESM2-WACCM-FV2: 'f', CMCC-CM2-SR5: 'g', CMCC-ESM2: 'h', CNRM-ESM2-1: 'i', CanESM5: 'j', CanESM5-CanOE: 'k', EC-Earth3-CC: 'l', EC-Earth3-Veg: 'm', EC-Earth3-Veg-LR: 'n', GISS-E2-1-G: 'o', HadGEM3-GC31-LL: 'p', HadGEM3-GC31-MM: 'q', INM-CM4-8: 'r', INM-CM5-0: 's', IPSL-CM5A2-INCA: 't', IPSL-CM6A-LR: 'u', MPI-ESM-1-2-HAM: 'v', MPI-ESM1-2-HR: 'w', UKESM1-0-LL: 'y'.

response to forest loss showed a strong sensitivity to the assumed increase in albedo with forest loss over a range of 0–0.09 ($9.0 \times 10^{-4} \%^{-1}$). However, they found forest loss reduced precipitation when the albedo sensitivity was greater than $3.0 \times 10^{-4} \%^{-1}$, opposite to our results of increased precipitation in models with greater brightening.

We note that the satellite-based sensitivity of albedo, ET and LAI to forest loss is less than would be expected based on *in-situ* measurements. In the Amazon, (Culf *et al* 1995) observed annual mean albedo of 0.13 for tropical forest and 0.18 for pasture, suggesting deforestation causes increased albedo of 0.05 or $4.6 \times 10^{-4} \%^{-1}$ (plotted as a red star in figures 4(a) and (d)), about a factor 4 greater than in the satellite measurements. *In-situ* data represents a complete conversion from forest to pasture with correspondingly large changes in albedo. In comparison, satellite data observes forest loss at larger scales where remaining tree cover and vegetation regrowth may reduce the change in albedo caused by forest loss. *In situ* observations of dry season ET in the Amazon are around $110 \text{ mm month}^{-1}$ for tropical forests and 70 mm month^{-1} for pasture (Restrepo-Coupe *et al* 2013), suggesting deforestation causes a reduction of

40 mm month^{-1} or $0.4 \text{ mm month}^{-1} \%^{-1}$ (plotted as a red star in figures 4(b) and (e)), around 3.5 times greater than seen in the satellite measurements. Challenges with remote-sensed ET data which combine remote sensed and model data (Baker *et al* 2021b) may explain the discrepancy with *in-situ* data. The simulated temperature response to forest loss is strongly related to albedo and ET in the dry season but less so in the wet season (Baker *et al* 2021b).

Our analysis focused on assessing the simulated local climate response to tropical deforestation and understanding how this depends on the modelled treatment of the land surface change. Tropical deforestation drives changes to the local energy balance that are dominated by changes in the turbulent energy flux (Boysen *et al* 2020, De Hertog *et al* 2023). Our analysis shows a large disagreement in the simulated response of ET flux to deforestation. However, uncertainty in measurements of the ET flux (Baker *et al* 2021b) are a challenge to constraining the simulated response of ET to forest loss. In contrast, satellite-derived datasets of surface albedo are more reliable (He *et al* 2014) and may provide a stronger constraint on the large spread of model simulated albedo responses to forest loss. We suggest that evaluating

and improving the surface albedo response to forest loss may be a logical and practical initial step to model improvement. Constraining the albedo sensitivity to deforestation is also important for accurate simulation of the radiative forcing due to historical land-use change (Lejeune *et al* 2020).

Previous work has shown that the climate response to deforestation depends on the background climate (Pitman *et al* 2011). To explore whether changes in background climate have changed the climate response to deforestation, we calculated how the simulated sensitivity of temperature to forest loss varied over the 1854–2014 period. We found that there was no significant trend in the simulated response of temperature to forest loss over this period (supplementary figure 12). The climate response to deforestation also depends on simulated atmospheric feedbacks through altering mesoscale circulations (Khanna *et al* 2017). Boysen *et al* (2020) found that increased shortwave radiation due to reduced cloud cover over regions of tropical deforestation was more important than changes in surface albedo in some models. Luo *et al* (2022) found mean reductions in ET over deforested areas (16.9 mm yr^{-1}) were about 4 times greater than reductions in mean flow convergence (-4.3 mm yr^{-1}), suggesting local reductions in ET dominate reduced rainfall rather than changes in circulation.

In addition to impacts on temperature and precipitation, deforestation can also impact other important climate variables such as causing reductions in low level cloud cover (Duveiller *et al* 2021). We focused on the local land surface warming due to forest loss, though we note that air temperature's response to deforestation may differ (Winckler *et al* 2019b). Deforestation can also cause important changes in the timing and intensity of precipitation. In Amazonia, deforestation has extended dry season and delayed the onset of the rainy season (Leite-Filho *et al* 2021, Commar *et al* 2023). In West Africa, deforestation has enhanced storm frequency (Taylor *et al* 2022). In addition to local impacts, deforestation may also change regional climate (Leite-Filho *et al* 2020). Tropical deforestation can cause reductions in downwind precipitation through reductions in moisture recycling (Spracklen *et al* 2012, Zemp *et al* 2017, Staal *et al* 2018) and can alter regional temperatures up to 50 km away from the location of land-use change (Cohn *et al* 2019). Deforestation may even alter precipitation in regions far removed from the land use change through teleconnections (Werth and Avissar 2005, Pitman *et al* 2009, De Noblet-Ducoudré *et al* 2012, Luo *et al* 2022).

4. Conclusions and implications

Our analysis provides further evidence of the local surface warming and drying (reduced precipitation) due to tropical deforestation. The multi-model mean

captures the observed surface warming due to tropical forest loss, with 22 out of 24 CMIP6 models analysed simulating warming in response to tropical forest loss. The multi-model mean suggests increased annual mean precipitation over regions of tropical forest loss, opposite in sign to the observed response. There is large variability in the magnitude of the modelled temperature and precipitation responses to deforestation, some of which we attribute to different implementations of land use change within CMIP6 models and the subsequent changes to albedo and ET. We find the simulated local land surface warming due to forest loss is sensitive to the simulated surface albedo change.

The local warming and drying due to tropical deforestation will have negative impacts on human health (Wolff *et al* 2018, Alves de Oliveira *et al* 2021), agriculture (Lawrence and Vandecar 2015, Leite-Filho *et al* 2021), surrounding forests (Zemp *et al* 2017, Staal *et al* 2020, Li *et al* 2022) and biodiversity (Pardini *et al* 2017). A warmer and drier climate will also exacerbate the risk of forest fires causing additional forest loss and the potential for positive climate feedbacks (Cochrane *et al* 1999). Some work has suggested the Amazon is close to a tipping point where additional deforestation would drive sufficient drying to induce forest dieback (Lovejoy and Nobre 2019). Future work is needed to assess the resilience of remaining tropical forests to a warmer and drier climate. Overall, our analysis provides additional impetus for policymakers to account for the local climate impacts of tropical deforestation (Duveiller *et al* 2020, Pongratz *et al* 2021).

Data availability statement

The dataset used in this analysis are all freely available through the following repositories: CMIP6 historical data from <https://esgf-index1.ceda.ac.uk/projects/cmip6-ceda/>, CHIRPS from <https://data.chc.ucsb.edu/products/?C=M;O=D>, CMORPH from https://ftp.cpc.ncep.noaa.gov/precip/CMORPH_RT/GLOBE/data/, GPCP from https://disc.gsfc.nasa.gov/datasets/GPCPMON_3.1/summary?keywords=GPCPMON, GPM from https://gpm1.gesdisc.eosdis.nasa.gov/data/GPM_L3/, PERSIANN (CCS, CDR, CCS-CDR, PDIR-NOW) from <https://chrsdata.eng.uci.edu/>, TRMM from https://disc.gsfc.nasa.gov/datasets/TRMM_3B43_7/summary, MODIS (MCD43A3, MOD16A2, MOD15A2, MOD11A2 and MCD12Q1) from <https://search.earthdata.nasa.gov/search> and Global Forest Change data from <https://storage.googleapis.com/earthenginepartners-hansen/GFC-2021-v1.9/download.html>.

Acknowledgments

The research has been supported by funding from the European Research Council (ERC) under the

European Union's Horizon 2020 research and innovation programme (DECAF project, Grant agreement No. 771492), and the Newton Fund, through the Met Office Climate Science for Service Partnership Brazil (CSSP Brazil). We also acknowledge that DIK was supported by the NC-International programme [NE/X006247/1] delivering National Capability. No competing interests. We acknowledge the World Climate Research Programme, which, through its Working Group on Coupled Modelling, coordinated and promoted CMIP6. We thank the climate modelling groups for producing and making available their model output, the Earth System Grid Federation (ESGF) for archiving the data and providing access, and the multiple funding agencies that support CMIP6 and ESGF.

Author contributions

J B downloaded and processed CMIP6 model data. JB and C S downloaded and processed MODIS observational data. C S downloaded and processed precipitation datasets. C S and J B analysed the data and designed and produced figures. All authors contributed to the design and editing of the manuscript.

Conflict of interest

The authors declare no competing interests.

ORCID iDs

Callum Smith  <https://orcid.org/0000-0002-2705-8398>

Robin Chadwick  <https://orcid.org/0000-0001-6767-5414>

Douglas I Kelley  <https://orcid.org/0000-0003-1413-4969>

Arthur P K Argles  <https://orcid.org/0000-0002-1346-6518>

Caio A S Coelho  <https://orcid.org/0000-0002-9695-5113>

Isabela L Talamoni  <https://orcid.org/0000-0003-4952-190X>

Dominick V Spracklen  <https://orcid.org/0000-0002-7551-4597>

Jessica C A Baker  <https://orcid.org/0000-0002-3720-4758>

References

- Alkama R and Cescatti A 2016 Biophysical climate impacts of recent changes in global forest cover *Science* **351** 600–4
- Alves de Oliveira B F, Bottino M J, Nobre P and Nobre C A 2021 Deforestation and climate change are projected to increase heat stress risk in the Brazilian Amazon *Commun. Earth Environ.* **2** 1–8
- Ashouri H, Hsu K L, Sorooshian S, Braithwaite D K, Knapp K R, Cecil L D, Nelson B R and Prat O P 2015 PERSIANN-CDR: daily precipitation climate data record from multisatellite observations for hydrological and climate studies *Bull. Am. Meteorol. Soc.* **96** 69–83
- Baker J C A, De Souza D C, Kubota P Y, Buermann W, Coelho C A S, Andrews M B, Gloor M, Garcia-Carreras L, Figueroa S N and Spracklen D V 2021a An assessment of land-atmosphere interactions over south America using satellites, reanalysis, and two global climate models *J. Hydrometeorol.* **22** 905–22
- Baker J C A, Garcia-Carreras L, Gloor M, Marsham J H, Buermann W, Da Rocha H R, Nobre A D, De Carioca Araujo A and Spracklen D V 2021b Evapotranspiration in the Amazon: spatial patterns, seasonality, and recent trends in observations, reanalysis, and climate models *Hydrol. Earth Syst. Sci.* **25** 2279–300
- Baker J C A and Spracklen D V 2019 Climate benefits of intact Amazon forests and the biophysical consequences of disturbance *Front. For. Glob. Change* **2** 1–13
- Berbet M L C and Costa M H 2003 Climate change after tropical deforestation: seasonal variability of surface albedo and its effects on precipitation change *J. Clim.* **16** 2099–104
- Boisier J P, Ciais P, Ducharne A and Guimberteau M 2015 Projected strengthening of Amazonian dry season by constrained climate model simulations *Nat. Clim. Change* **5** 656–60
- Bonan G B 2008 Forests and climate change: forcings, feedbacks, and the climate benefits of forests *Science* **320** 1444–9
- Boucher O et al 2018 IPSL IPSL-CM6A-LR model output prepared for CMIP6 CMIP historical *Earth System Grid Federation* (<https://doi.org/10.22033/ESGF/CMIP6.5195>)
- Boysen L R et al 2020 Global climate response to idealized deforestation in CMIP6 models *Biogeosciences* **17** 5615–38
- Bright R M, Davin E, O'Halloran T, Pongratz J, Zhao K and Cescatti A 2017 Local temperature response to land cover and management change driven by non-radiative processes *Nat. Clim. Change* **7** 296–302
- Cochrane M A, Alencar A, Schulze M D, Souza C M, Nepstad D C, Lefebvre P and Davidson E A 1999 Positive feedbacks in the fire dynamic of closed canopy tropical forests *Science* **284** 1832–5
- Cohn A S, Bhattarai N, Campolo J, Crompton O, Dralle D, Duncan J and Thompson S 2019 Forest loss in Brazil increases maximum temperatures within 50 km *Environ. Res. Lett.* **14** 084047
- Commar L F S, Abrahão G M and Costa M H 2023 A possible deforestation-induced synoptic-scale circulation that delays the rainy season onset in Amazonia *Environ. Res. Lett.* **18** 044041
- Costa M H, Yanagi S N M, Souza P J O P, Ribeiro A and Rocha E J P 2007 Climate change in Amazonia caused by soybean cropland expansion, as compared to caused by pastureland expansion *Geophys. Res. Lett.* **34** 2–5
- Culf A D, Fisch G and Hodnett M G 1995 The albedo of Amazonian forest and ranch land *J. Clim.* **9** 1544–54
- Danabasoglu G 2019a NCAR CESM2 model output prepared for CMIP6 CMIP historical *Earth System Grid Federation* (<https://doi.org/10.22033/ESGF/CMIP6.10023>)
- Danabasoglu G 2019b NCAR CESM2-FV2 model output prepared for CMIP6 CMIP historical *Earth System Grid Federation* (<https://doi.org/10.22033/ESGF/CMIP6.11281>)
- Danabasoglu G 2019c NCAR CESM2-WACCM model output prepared for CMIP6 CMIP historical *Earth System Grid Federation* (<https://doi.org/10.22033/ESGF/CMIP6.10023>)
- Danabasoglu G 2019d NCAR CESM2-WACCM-FV2 model output prepared for CMIP6 CMIP historical *Earth System Grid Federation* (<https://doi.org/10.22033/ESGF/CMIP6.11282>)
- Danek C, Shi X, Stepanek C, Yang H, Barbi D, Hegewald J and Lohmann G 2020 AWI AWI-ESM1.1LR model output prepared for CMIP6 CMIP historical *Earth System Grid Federation* (<https://doi.org/10.22033/ESGF/CMIP6.9301>)

- Davin E L and de Noblet-ducouudre N 2010 Climatic impact of global-scale deforestation: radiative versus nonradiative processes *J. Clim.* **23** 97–112
- De Hertog S J *et al* 2023 The biogeophysical effects of idealized land cover and land management changes in Earth system models *Earth Syst. Dyn.* **14** 629–67
- De Noblet-Ducoudré N *et al* 2012 Determining robust impacts of land-use-induced land cover changes on surface climate over North America and Eurasia: results from the first set of LUCID experiments *J. Clim.* **25** 3261–81
- Dirmeyer P A and Shukla J 1994 Albedo as a modulator of climate response to tropical deforestation *J. Geophys. Res.* **99** 20863–77
- Duveiller G, Caporaso L, Abad-Viñas R, Perugini L, Grassi G, Arneith A and Cescatti A 2020 Local biophysical effects of land use and land cover change: towards an assessment tool for policy makers *Land Use Policy* **91** 1–11
- Duveiller G, Filipponi F, Ceglár A, Bojanowski J, Alkama R and Cescatti A 2021 Revealing the widespread potential of forests to increase low level cloud cover *Nat. Commun.* **12** 1–15
- Duveiller G, Hooker J and Cescatti A 2018 The mark of vegetation change on Earth's surface energy balance *Nat. Commun.* **9** 1–12
- EC-Earth-Consortium 2019 EC-Earth-Consortium EC-Earth3-Veg model output prepared for CMIP6 CMIP historical *Earth System Grid Federation* (<https://doi.org/10.22033/ESGF/CMIP6.692>)
- EC-Earth-Consortium 2020 EC-Earth-Consortium EC-Earth3-Veg-LR model output prepared for CMIP6 CMIP historical *Earth System Grid Federation* (<https://doi.org/10.22033/ESGF/CMIP6.643>)
- EC-Earth-Consortium 2021 EC-Earth-Consortium EC-Earth-3-CC model output prepared for CMIP6 CMIP historical *Earth System Grid Federation* (<https://doi.org/10.22033/ESGF/CMIP6.4702>)
- Friedl M and Sulla-Menashe D 2022 MODIS/Terra+ Aqua land cover type yearly L3 global 500m SIN Grid V061 NASA EOSDIS Land Processes DAAC (<https://doi.org/10.5067/MODIS/MCD12Q1.061>) (Accessed 1 January 2022)
- Funk C *et al* 2015 The climate hazards infrared precipitation with stations—a new environmental record for monitoring extremes *Sci. Data* **2** 1–21
- Garcia-Carreras L and Parker D J 2011 How does local tropical deforestation affect rainfall? *Geophys. Res. Lett.* **38** 1–6
- Hansen M C *et al* 2013 High-resolution global maps of 21st-century forest cover change *Science* **342** 850–3
- He T, Liang S and Song D-X 2014 Analysis of global land surface albedo climatology and spatial-temporal variation during 1981–2010 from multiple satellite products *J. Geophys. Res. Atmos.* **119** 10,281–98
- Hou A Y, Kakar R K, Neeck S, Azarbarzin A A, Kummerow C D, Kojima M, Oki R, Nakamura K and Iguchi T 2014 The global precipitation measurement mission *Bull. Am. Meteorol. Soc.* **95** 701–22
- Huffman G J A, Behrangi R F, Adler D T, Bolvin E J and Nelkin G G 2022 *Introduction to the New Version 3 GPCP Monthly Global Precipitation Analysis* (available at: https://docsserver.gesdisc.eosdis.nasa.gov/public/project/MEaSURES/GPCP/Release_Notes.GPCPV3.2.pdf)
- Huffman G J, Adler R F, Bolvin D T, Gu G, Nelkin E J, Bowman K P, Hong Y, Stocker E F and Wolff D B 2007 The TRMM multisatellite precipitation analysis (TMPA): quasi-global, multiyear, combined-sensor precipitation estimates at fine scales *J. Hydrometeorol.* **8** 38–55
- Jungclaus J *et al* 2019 MPI-M MPI-ESM1.2-HR model output prepared for CMIP6 CMIP historical *Earth System Grid Federation* (<https://doi.org/10.22033/ESGF/CMIP6.762>)
- Khanna J, Medvigy D, Fueglistaler S and Walko R 2017 Regional dry-season climate changes due to three decades of Amazonian deforestation *Nat. Clim. Change* **7** 200–4
- Kumar S, Dirmeyer P A, Merwade V, Delsole T, Adams J M and Niyogi D 2013 Land use/cover change impacts in CMIP5 climate simulations: a new methodology and 21st century challenges *J. Geophys. Res. Atmos.* **118** 6337–53
- Lawrence D and Vandecar K 2015 Effects of tropical deforestation on climate and agriculture *Nat. Clim. Change* **5** 27–36
- Lee X *et al* 2011 Observed increase in local cooling effect of deforestation at higher latitudes *Nature* **479** 384–7
- Leite-Filho A T, Costa M H and Fu R 2020 The southern Amazon rainy season: the role of deforestation and its interactions with large-scale mechanisms *Int. J. Climatol.* **40** 2328–41
- Leite-Filho A T, Soares-Filho B S, Davis J L, Abrahão G M and Börner J 2021 Deforestation reduces rainfall and agricultural revenues in the Brazilian Amazon *Nat. Commun.* **12** 1–7
- Lejeune Q, Davin E L, Duveiller G, Crezee B, Meier R, Cescatti A and Seneviratne S I 2020 Biases in the albedo sensitivity to deforestation in CMIP5 models and their impacts on the associated historical radiative forcing *Earth Syst. Dyn.* **11** 1209–32
- Lejeune Q, Seneviratne S I and Davin E L 2017 Historical land-cover change impacts on climate: comparative assessment of LUCID and CMIP5 multimodel experiments *J. Clim.* **30** 1439–59
- Li Y, Brando P M, Morton D C, Lawrence D M, Yang H and Randerson J T 2022 Deforestation-induced climate change reduces carbon storage in remaining tropical forests *Nat. Commun.* **13** 1–13
- Li Y, Zhao M, Motesharrei S, Mu Q, Kalnay E and Li S 2015 Local cooling and warming effects of forests based on satellite observations *Nat. Commun.* **6** 1–8
- Lovato T and Peano D 2020 CMCC CMCC-CM2-SR5 model output prepared for CMIP6 CMIP historical *Earth System Grid Federation* (<https://doi.org/10.22033/ESGF/CMIP6.3825>)
- Lovato T, Peano D and Butenschön M 2021 CMCC CMCC-ESM2 model output prepared for CMIP6 CMIP historical *Earth System Grid Federation* (<https://doi.org/10.22033/ESGF/CMIP6.13164>)
- Lovejoy T E and Nobre C 2019 Amazon tipping point: last chance for action *Sci. Adv.* **5** 4–6
- Luo X, Ge J, Guo W, Fan L, Chen C, Liu Y and Yang L 2022 The biophysical impacts of deforestation on precipitation: results from the CMIP6 model intercomparison *J. Clim.* **35** 3293–311
- Met Office 2023 Iris: a powerful, format-agnostic, and community-driven Python package for analysing and visualising Earth science data (available at: <http://scitools.org.uk/>)
- Myneni R, Knyazikhin Y and Park T 2021 MODIS/Terra Leaf Area Index/FPAR 8-Day L4 Global 500m SIN Grid V061 NASA EOSDIS Land Processes DAAC (<https://doi.org/10.5067/MODIS/MOD15A2H.061>)
- NASA/GISS 2018 NASA-GISS GISS-E2.1G model output prepared for CMIP6 CMIP historical *Earth System Grid Federation* (<https://doi.org/10.22033/ESGF/CMIP6.1400>)
- Neubauer D *et al* 2019 HAMMOZ-Consortium MPI-ESM1.2-HAM model output prepared for CMIP6 CMIP historical *Earth System Grid Federation* (<https://doi.org/10.22033/ESGF/CMIP6.1622>)
- Nguyen P *et al* 2019 The CHRS data portal, an easily accessible public repository for PERSIANN global satellite precipitation data *Sci. Data* **6** 1–10
- Pardini R, Nichols L and Püttker T 2017 Biodiversity response to habitat loss and fragmentation *Encyclopedia of the Anthropocene* vol 3 (Elsevier) pp 229–39
- Pitman A J *et al* 2009 Uncertainties in climate responses to past land cover change: first results from the LUCID intercomparison study *Geophys. Res. Lett.* **36** 1–6
- Pitman A J, Avila F B, Abramowitz G, Wang Y P, Phipps S J and De Noblet-Ducoudré N 2011 Importance of background climate in determining impact of land-cover change on regional climate *Nat. Clim. Change* **1** 472–5
- Pongratz J, Schwingshackl C, Bultan S, Obermeier W, Havermann F and Guo S 2021 Land use effects on climate:

- current state, recent progress, and emerging topics *Curr. Clim. Change Rep.* **7** 99–120
- Restrepo-Coupe N et al 2013 What drives the seasonality of photosynthesis across the Amazon basin? A cross-site analysis of eddy flux tower measurements from the Brasil flux network *Agric. For. Meteorol.* **182–183** 128–44
- Ridley J, Menary M, Kuhlbrodt T, Andrews M and Andrews T 2019 MOHC HadGEM3-GC31-MM model output prepared for CMIP6 CMIP historical *Earth System Grid Federation* (<https://doi.org/10.22033/ESGF/CMIP6.420>)
- Robertson E 2019 The local biophysical response to land-use change in HADGEM2-ES *J. Clim.* **32** 7611–27
- Running S, Mu Q, Zhao M and Moreno A 2021 MODIS/terra net evapotranspiration gap-filled 8-day L4 global 500m SIN grid V061 *NASA EOSDIS Land Processes DAAC* (<https://doi.org/10.5067/MODIS/MOD16A2GE061>)
- Sadeghi M, Nguyen P, Naeini M R, Hsu K, Braithwaite D and Sorooshian S 2021 PERSIANN-CCS-CDR, a 3-hourly 0.04° global precipitation climate data record for heavy precipitation studies *Sci. Data* **8** 1–11
- Schaaf C and Wang Z 2021 MODIS/terra+ aqua BRDF/albedo daily L3 global—500m V061 *NASA EOSDIS Land Processes DAAC* (<https://doi.org/10.5067/MODIS/MCD43A3.061>)
- Seferian R 2018 CNRM-CERFACS CNRM-ESM2-1 model output prepared for CMIP6 CMIP historical *Earth System Grid Federation* (<https://doi.org/10.22033/ESGF/CMIP6.4068>)
- Smith C, Baker J C A and Spracklen D V 2023 Tropical deforestation causes large reductions in observed precipitation *Nature* **615** 270–5
- Spracklen D V, Arnold S R and Taylor C M 2012 Observations of increased tropical rainfall preceded by air passage over forests *Nature* **489** 282–5
- Spracklen D V and Garcia-Carreras L 2015 The impact of Amazonian deforestation on Amazon basin rainfall *Geophys. Res. Lett.* **42** 9546–52
- Staal A, Flores B M, Aguiar A P D, Bosmans J H C, Fetzer I and Tuinenburg O A 2020 Feedback between drought and deforestation in the Amazon *Environ. Res. Lett.* **15** 044024
- Staal A, Tuinenburg O A, Bosmans J H C, Holmgren M, Van Nes E H, Scheffer M, Zemp D C and Dekker S C 2018 Forest-rainfall cascades buffer against drought across the Amazon *Nat. Clim. Change* **8** 539–43
- Swart N C et al 2019a CCCma CanESM5 model output prepared for CMIP6 CMIP historical *Earth System Grid Federation* (<https://doi.org/10.22033/ESGF/CMIP6.1301>)
- Swart N C et al 2019b CCCma CanESM5-CanOE model output prepared for CMIP6 CMIP historical *Earth System Grid Federation* (<https://doi.org/10.22033/ESGF/CMIP6.10205>)
- Tang Y, Rumbold S, Ellis R, Kelley D, Mulcahy J, Sellar A, Walton J and Jones C 2019 MOHC UKESM1.0-LL model output prepared for CMIP6 CMIP historical *Earth System Grid Federation* (<https://doi.org/10.22033/ESGF/CMIP6.6113>)
- Taylor C M, Klein C, Parker D J, Gerard F, Semeena V S, Barton E J and Harris B L 2022 “Late-stage” deforestation enhances storm trends in coastal West Africa *Proc. Natl Acad. Sci.* **119** 1–8
- Vancutsem C, Achard F, Pekel J F, Vieilledent G, Carboni S, Simonetti D, Gallego J, Aragão L E O C and Nasi R 2021 Long-term (1990–2019) monitoring of forest cover changes in the humid tropics *Sci. Adv.* **7** 1–22
- Virtanen P et al 2020 {SciPy} 1.0: fundamental algorithms for scientific computing in python *Nat. Methods* **17** 261–72
- Volodin E et al 2019a NM INM-CM4-8 model output prepared for CMIP6 CMIP historical *Earth System Grid Federation* (<https://doi.org/10.22033/ESGF/CMIP6.1422>)
- Volodin E et al 2019b NM INM-CM5-0 model output prepared for CMIP6 CMIP historical *Earth System Grid Federation* (<https://doi.org/10.22033/ESGF/CMIP6.1423>)
- Wan Z, Hook S and Hulley G 2021 MODIS/terra land surface temperature/emissivity 8-day L3 global 1km SIN grid V061 *NASA EOSDIS Land Processes DAAC* (<https://doi.org/10.5067/MODIS/MOD11A2.061>)
- Werth D and Avissar R 2005 The local and global effects of African deforestation *Geophys. Res. Lett.* **32** 1–4
- Winckler J, Reick C H, Bright R M and Pongratz J 2019a Importance of surface roughness for the local biogeophysical effects of deforestation *J. Geophys. Res.* **124** 8605–18
- Winckler J, Reick C H and Pongratz J 2017 Robust identification of local biogeophysical effects of land-cover change in a global climate model *J. Clim.* **30** 1159–76
- Winckler J, Reick, Christian H, Luyssaert S, Cescatti A, Stoy P C, Lejeune Q, Raddatz T, Chlond A, Heidkamp M and Pongratz J 2019b Different response of surface temperature and air temperature to deforestation in climate models *Earth Syst. Dyn.* **10** 473–84
- Windisch M G, Davin E L and Seneviratne S I 2021 Prioritizing forestation based on biogeochemical and local biogeophysical impacts *Nat. Clim. Change* **11** 867–71
- Wolff N H, Masuda Y J, Meijaard E, Wells J A and Game E T 2018 Impacts of tropical deforestation on local temperature and human well-being perceptions *Glob. Environ. Change* **52** 181–9
- Xie P, Joyce R, Wu S, Yoo S-H, Yarosh Y, Sun F and Lin R 2019 NOAA climate data record (CDR) of CPC morphing technique (CMORPH) high resolution global precipitation estimates, version 1 NOAA *National Centers for Environmental Information* (<https://doi.org/10.25921/w9va-q159>)
- Zemp D C, Schleussner C F, Barbosa H M J, Hirota M, Montade V, Sampaio G, Staal A, Wang-Erlandsson L and Rammig A 2017 Self-amplified Amazon forest loss due to vegetation-atmosphere feedbacks *Nat. Commun.* **8** 1–10
- Zhuang J 2022 xESMF (<https://doi.org/10.5281/zenodo.1134365>)
- Ziehn T et al 2019 CSIRO ACCESS-ESM1.5 model output prepared for CMIP6 CMIP historical *Earth System Grid Federation* (<https://doi.org/10.22033/ESGF/CMIP6.4272>)